Reactive power minimization of dual active bridge DC/DC converter with triple phase shift control using neural network

Harrye, Yasen A.; Ahmed, Khaled; Aboushady, Ahmed

Published in:
2014 International Conference on Renewable Energy Research and Application (ICRERA)

DOI:
10.1109/ICRERA.2014.7016448

Publication date:
2014

Document Version
Author accepted manuscript

Reactive Power Minimization of Dual Active Bridge DC/DC Converter with Triple Phase Shift Control using Neural Network

Yasen A. Harrye & Khaled H. Ahmed
School of Engineering, University of Aberdeen
Aberdeen, U.K
yasen.harrye@abdn.ac.uk

Ahmed A. Aboushady
School of Engineering, University of Aberdeen, UK
On leave from Arab Academy for Science & Technology
Alexandria, Egypt

Abstract—**Reactive power flow increases dual active bridge (DAB) converter RMS current leading to an increase in conduction losses especially in high power applications. This paper proposes a new optimized triple phase shift (TPS) switching algorithm that minimizes the total reactive power of the converter. The algorithm iteratively searches for TPS control variables that satisfy the desired active power flow while selecting the operating mode with minimum reactive power consumption. This is valid for the whole range of converter operation. The iterative algorithm is run offline for the entire active power range (-1pu to 1pu) and the resulting data is used to train an open loop artificial neural network controller to reduce computational time and memory allocation necessary to store the data generated. To validate the accuracy of the proposed controller, a 500-MW 300kV/100kV DAB model is simulated in Matlab/Simulink, as a potential application for DAB in DC grids.**

Keywords- DC-DC converter, Dual active bridge (DAB) converter, Neural network (NN) controller, Reactive power, Triple phase shift (TPS).

I. INTRODUCTION

High power DC-DC converters are recently becoming indispensable in areas of high power DC grids and renewable energy generation [1, 2]. This has been driven mainly by the need to interconnect different offshore wind farm clusters that are geographically separated in order to transmit power to onshore population centers, the anticipated European super grid and the need to offload congested/aging AC grids as demonstrated in Fig. 1. In DC power transmission, the challenges have been maintaining the reliability and security of DC lines. Protection, fault isolation, voltage regulation, power flow control, and interconnections of different medium power lines using efficient DC-DC converters has been subject of investigation recently [1]. In renewable energy generation such as wind and solar, due their spasmodic nature, energy storage system is required to store energy during high generation peaks and retrieve during low peaks, hence the need to use bidirectional DC-DC converters [3].

In this paper isolated bidirectional dual active bridge converter (DAB) [4] is studied for its potential application in DC grids. Its desirable features for use in high power applications include low number of passive components,

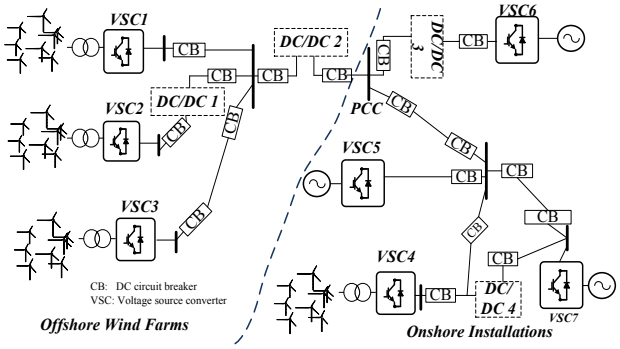

Fig. 1. DC-DC converters application in DC Grid

galvanic isolation, soft switching ability, bidirectional power flow, high power density and possibility of high stepping ratio of conversion. Recent research in DAB has been mainly focused on facilitation of efficiency improvement through accurate modelling [5-7], use of low loss switching devices [8], circuit topology and modulations schemes of the converter [9-17]. DAB modulations scheme are an active area of research and involves optimizing existing modulations schemes so that converter losses are minimized. Several modulation schemes have been proposed in literature, including conventional phase shift (CPS) modulation [9], Dual phase shift (DPS) modulation [10,11], extended phase shift (EPS) modulation [12], Triple phase shift (TPS) modulation [13-15], Pulse width modulation (PWM) [16,17] and hybrids of some of the above.

CPS modulation operates the converter transformer voltages with full square waves while controlling their respective phase shifts to control active power flow. Whilst this control method is simple to implement, it results in high circulating current, limited soft switching range and inability of reactive power control. To resolve this, DPS was proposed to reduce the converter circulating current and eliminate/reduce reactive power. This is achieved by introducing zero states in the transformer voltages through additional inner phase shift between the converter legs. But as pointed out in [16], there are sub-optimal modes of operation within this scheme. Similarly, in [12] attempts are made to reduce converter circulating power by introducing EPS control scheme which is

a special case of DPS. Both [10,12], define reactive power flow within the converter as a backflow power. This definition is inaccurate because it means that reactive power only occurs when the voltage and current are of opposite polarity (negative power flow). TPS control adds another degree of freedom to DPS scheme by introducing an extra control parameter in the modulation with the aim of increasing ZVS soft switching range and increasing overall DAB efficiency. In [15], a multi-phase shift approach of DPS and TPS was investigated so as to determine optimal sub modes from the transformer voltage waveforms. Pulse width modulation (PWM) for DAB has been addressed in detail by [16]. Using single PWM, Dual PWM and hybrid combinations of CPS and PWM, the authors have shown an improvement in low power operation of the converter in wide input-output voltages, extension of ZVS range, reduction of peak and RMS currents and further reduction of the transformer size by using high frequency switching. In [17], an extension of ZVS of the converter was investigated using PWM.

This paper is an extension of work in [18] and proposes a new DAB reactive power optimization algorithm based on TPS modulation that is implemented using an open loop neural network controller. In contrast to previous publications, that defined reactive power as back flow power, reactive power flow is defined as true reactive power consumption by the DAB inductor with no fundamental frequency approximation of the voltages and current as in [16,19]. Due to the existence of three degrees of freedom in controlling active power flow in TPS modulation, this makes application of linear PI control to DAB converter not possible. Therefore, an iterative optimization algorithm technique is used instead to search in all the derived power equations [18] for TPS control variables that satisfy user defined reference active power with minimum level of reactive power absorption. For real time implementation, this iterative optimization algorithm is time consuming, so an offline set of data is generated from the search results. This data set is used to train a neural network (NN) controller which is simple to implement, fast and does not require a large memory allocation.

The structure of the rest of the paper is as follows. DAB converter topology under TPS control and the iterative reactive power optimization algorithm are discussed in section II. Implementation of NN controller is explained in section III. In order to validate the performance of the algorithm, results are given in section IV. In section V, conclusions of the important points in this paper are noted.

II. HIGH POWER DAB CONVERTER

A. Converter analysis using triple phase Shift control

Bidirectional DAB circuit topology is depicted in Fig. 2(a) and it comprises two H-bridges, external inductor L_{ext}, to facilitate power transfer and a high frequency isolation transformer. By referring the converter to the transformer primary side, neglecting transformer magnetizing inductance, adding transformer leakage inductance to the external inductor

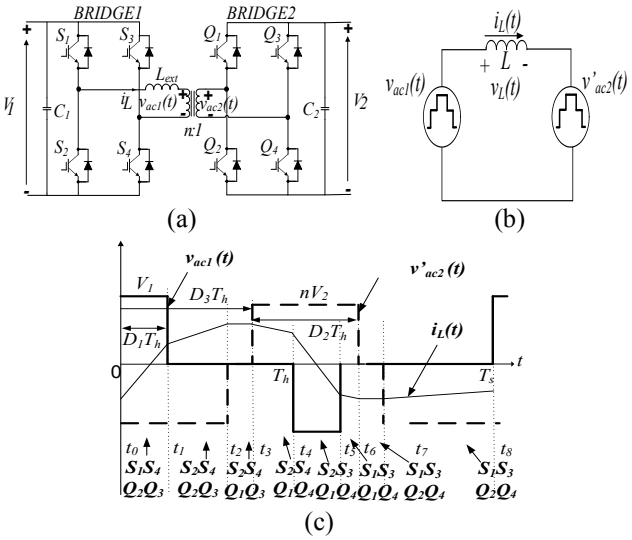

Fig. 2. (a) DAB circuit diagram (b) Simplified model with secondary side of transformer referred to the primary (c) Ideal voltage & current waveforms using TPS

(L_{ext}) to form L, and with *n:1* transformer turns ratio, circuit of Fig. 2 (a), can be simplified to its AC equivalent circuit model in Fig.2 (b). With TPS, three parameters D_1, D_2 and D_3 are used to control the converter bridges. D_1 is the inner phase shift between switches S_1 & S_4, D_2 is the inner phase shift between the switches Q_1 & Q_4 while D_3 is the outer phase shift between S_1 & Q_1 as illustrated in Fig. 2(c). Based on combinations of phase shifts D_1, D_2 and D_3, full, partial and no overlaps of both bridges quasi square wave voltages give rise to six switching modes and their complements, for both power flow directions using TPS and the operating waveforms for each of these modes are illustrated in Fig. 3 [18].

B. Reactive power minimization algorithm

By minimizing reactive power flow, RMS inductor /transformer current is reduced, resulting in converter conduction loss reduction. In [18], reactive power is computed by calculating the apparent power S_L at the inductor. Since inductors do not absorb active power, the apparent power is therefore equivalent to the reactive power consumption by the inductor. Using the simplified circuit model in Fig. 2(b), the converter total reactive power expression for all modes were computed [18] and derived using the expression,

$$Q = S_L = V_{L_{RMS}} I_{L_{RMS}} \tag{1}$$

To meet the desired level of active power transfer by the DAB, several modes of operation, with different combinations of TPS control variables can be used. Each TPS combination although satisfies the desired active power level, generates a different level of reactive power consumption. An iterative optimization technique implementing the steady state active and reactive power equations [18] repetitively searches for the three TPS control parameters, D_1, D_2 & D_3 which satisfy the reference power order and selects the combinations of the control variables that meet the minimum true reactive power

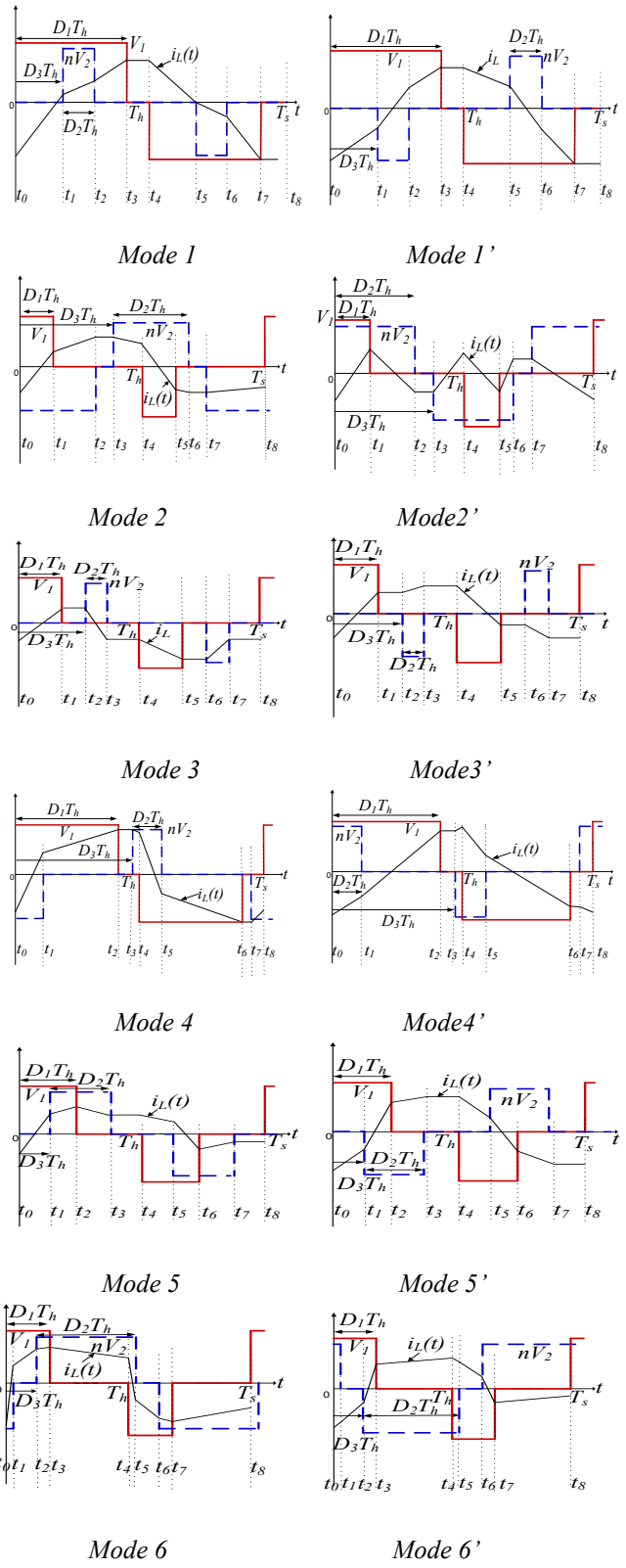

Fig. 3. TPS control modes of operation [18]

consumption using all the modes listed in Fig. 3. A flow chart of the procedure is illustrated in Fig. 4. The steps for optimizing for minimum reactive power can be summarized

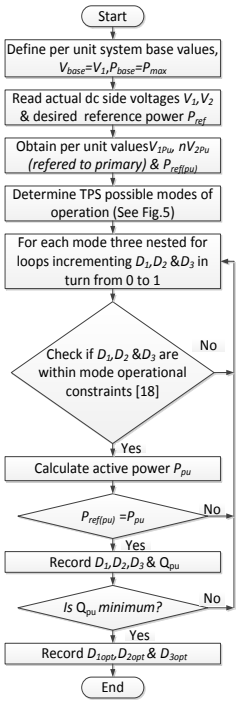

Fig. 4. Flow chart of the proposed TPS iterative optimization algorithm

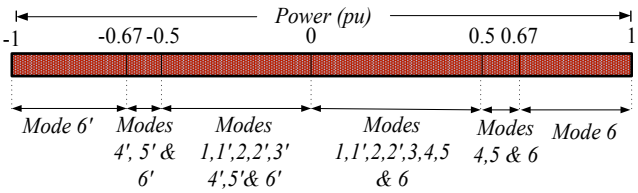

Fig. 5. Map of TPS modes vs output power ranges in pu

as follows.

- Determination of modes that meet the required reference output power ($P_{ref(pu)}$) as Fig. 5 shows.
- Once the correct modes are determined, calculate active power
- The minimum reactive power consumption using expressions defined in [18] is evaluated.
- Finally respective values of D_1, D_2 & D_3 are generated for the optimum mode (D_{1opt}, D_{2opt} & D_{3opt})

III. NEURAL NETWORK BASED CONTROLLER

The algorithm discussed in section II involves iterative searching of the optimum TPS variables as Fig. 4 illustrated. In real time, depending on the microcontroller speed and memory size, this can be computationally intensive. Therefore, to solve this, the algorithm is run offline in Matlab and data is collated for the entire active power range (-1 p.u to 1 p.u). This data is used in training an open loop NN controller which improves the computational speed of the algorithm due to its parallel input data processing capability and once trained, generates TPS variables for the DAB under any operating conditions.

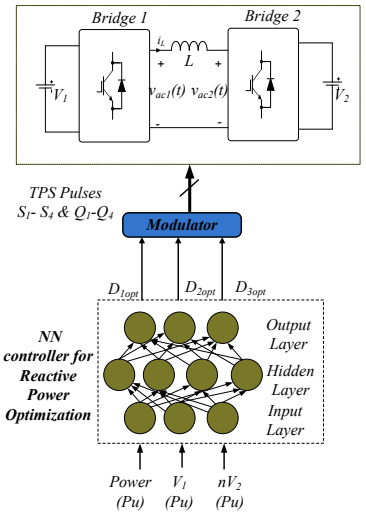

Fig. 6. Implementation of reactive power minimization algorithm using NN controller

Multilayer feed forward neural networks consist of input layer, hidden layer, and output layer as illustrated in Fig. 6. These layers are connected by synapses of weights that either increase or decrease the input signals before they are summed and passed through transfer function. Weights and the biases of the network are tuned in incremental or batch mode by using numerical optimization algorithms that compute either the Jacobian of the network error or the gradient of the network performance with respect to the weights using back-propagation algorithm [20]. By iteratively tuning the weights and biases, the network is optimized depending on the performance requirements. In feed forward neural networks, mean square error (*MSE*) between the outputs of the network and the target outputs is mainly used cost function.

The training is performed using 214 input and output data points consisting of per unit reference power ($P_{ref\,(pu)}$), and DC link voltages V_{1pu} and nV_{2pu}. The target data is the corresponding optimized TPS control variables (D_{1opt}, D_{2opt} & D_{3opt}) for minimum reactive power output.

A structure of 3 inputs, 20 hidden and 3 output layers was used to batch train the network using the process of Bayesian regularization [21] and a hyperbolic tangent (tan-sigmoid) activation functions for both hidden and output layers was used since the data range is between 1 and -1. Bayesian regularization process uses Levenberg-Marquardt numerical optimization algorithm [22] to train the network in order to generalize and prevent over fitting of data through jointly minimizing the weights and sum squared errors [20]. Therefore, during training, the weights & biases are tuned iteratively and updated for all layers until a satisfactory performance value was obtained after 120 epochs using sum squared error (SSE) performance function. Fig. 7 shows the regression plots of the data (Y) and target (T). The correlation coefficient R is equal to 99.7% and indicates how well the network has fitted the data.

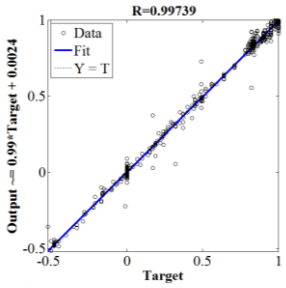

Fig. 7. Regression plot of output vs target data

IV. PERFORMANCE EVALUATION OF THE ALGORITHM

To substantiate the analysis presented, detailed simulations using Matlab/Simulink was performed using a converter specification of 500 MW, DC link voltages of 300kV/100kV, a 500 Hz switching frequency and DAB inductor of 45mH.

A. Rated power, power reversal and partial power operation

Results in Fig.8, show the response of the converter to changes in the active power. In Fig. 8 (a), the active power reference of the converter is set at full rating (1 p.u) at t=0. At time t=0.2s, a step full power reversal is undertaken to -1 p.u and at t=0.4*s*, active power is stepped back to 1 p.u. Afterwards, a partial power operation of the converter is demonstrated from 1 p.u to 0.5 p.u at t=0.6s and 0.25 p.u at time t=0.8s. This shows that the converter can operate at rated and partial power with fast transient response thanks to the NN controller. Fig.8 (b) illustrates the converter true reactive power. At rated maximum active power of 1 p.u and -1 p.u, the reactive power is uncontrollable and has a maximum value of Q=2.3 p.u. Therefore the NN controller works when $|P_{pu}|<1$ p.u which is apparent at t>0.6s. This is discussed in more detail in the next subsection. The AC voltages and currents at 500 Hz are depicted in Fig. 8 (c). It can be observed that the transformer AC voltages v_{ac1} and v_{ac2}, are full square waves during the 1 p.u active power transfer with 90^0 phase shift which corresponds to the case of conventional phase shift control. During 0.25 p.u power transfer, v_{ac1} and v_{ac2}, are nearly in phase allowing reduced power flow from bridge 1 to bridge 2. The current i_L reduction during partial power operation of 0.5 p.u and 0.25 p.u is evident in Fig 8 (d). Fig 8(e) shows optimum TPS control variables generated by the open loop algorithm as a result of changes in the power reference.

B. Minimum reactive power selection

Table I, shows the effectiveness of the iterative algorithm in choosing minimum reactive power (Q_{min}). At partial loading of 0.25 p.u and 0.50 p.u, eight different modes meet the active power requirement as depicted in Fig. 5. When $P_{ref\,(pu)=}$ 0.25pu, a Q_{min} of 0.10 p.u for both modes *5 & 6* results, while modes 1' & 2 generate the maximum reactive power (Q_{max}) flow of 1.51 p.u with a difference of 1.41p.u for the same active power requirement. Similarly at partial loading of $P_{ref\,(pu)=}$0.5p.u, the efficiency of the algorithm is even more noticeable. Modes 5 & *6* results in a Q_{min} of 0.34 p.u whilst mode 1', has Q_{max}=2.78 p.u, with a difference of 2.44 p.u. These minimum reactive

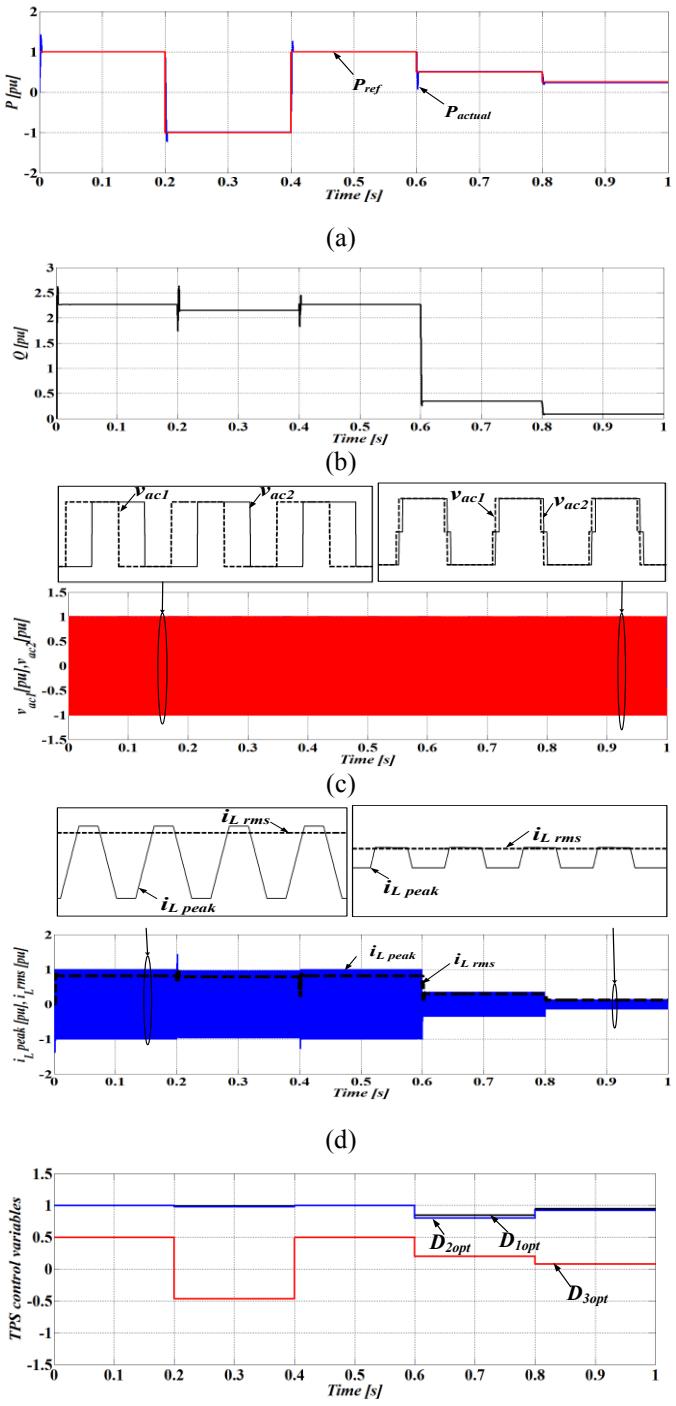

Fig. 8. Waveforms demonstrating DAB response to proposed minimal reactive power NN controller (a) active power (b) reactive power, (c) voltage waveforms for bridges 1 & 2, (d) inductor current, (e) optimum TPS control variables D_{1opt},D_{2opt} and D_{3opt}

power values are the optimum selected values by the controller and are shown in Fig. 8 (b).

C. DAB DC faults ride through capability

Investigation of DAB fault current characteristics and fault ride through capability is vital for high power applications. Pole to pole DC fault shown in Fig. 9 is the most severe and is

Table I**:** Reactive power selection using iterative algorithm

Power ($P_{ref(pu)}$)	*0.5pu*	*0.25pu*
Possible modes *(see Fig. 5)*	*1,1',2,2',3,4,5 & 6*	*1,1',2,2'3,4,5 & 6*
Modes reactive power (pu) *(Minimum selected in bold font)*	*Q_1=0.55,$Q_{1'}$=2.78, Q_2=2.77,$Q_{2'}$=0.54, Q_3=1.14,Q_4=1.14,* ***Q_5=0.34, Q_6=0.34***	*Q_1=0.11,$Q_{1'}$=1.51, Q_2=1.51,$Q_{2'}$=0.12, Q_3=0.58,Q_4=0.86,* ***Q_5=0.10, Q_6=0.10***

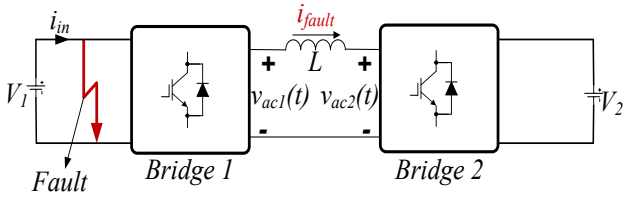

Fig. 9. Illustration of pole-pole DC fault on V_1 side

seen as an AC fault by non-faulted side bridge. Therefore as long as RMS fault current is within twice RMS rated current, IGBTs can yet be used to switch the fault current allowing to control it and there is no need to trip/ block IGBTs.

Fig. 10 shows DAB response with the proposed NN controller under DC faults. Initially the converter is assumed to be operating at full rated power before the fault is applied. At time t=0.2s a temporary pole to pole DC fault is introduced and cleared at t=0.4s. Fig. 10 (a) demostrates that during the fault the active power drops to zero and bridge 2 only supplies reactive power to the DAB inductor as shown in Fig. 10 (b). Fig. 10 (c) & (d) show the AC voltages. Reduction of voltage v_{ac1} to zero can be noticed due to the fault while voltage v_{ac2} remains unaffected during the fault. The fault current peak is the same compared to rated operation with a reduction in RMS value during the fault as portrayed in Fig. 10 (e). This is significant advantage of DAB where fault current is less than rated current due to absence of opposite polarity AC voltages during the fault which increases total resultant voltage across DAB inductor leading to higher currents. For this reason, no control action is necessary from the non-faulted side bridge (bridge 2) to limit fault current and no external DC circuit breakers are needed as well.

V. CONCLUSIONS

Reactive power minimization algorithm using TPS control scheme was presented for high power DAB converter. By iteratively searching for the optimum TPS variables, it has been shown that reactive power consumption can be significantly reduced for partial active power operation. Neural network controller was trained using data from the iterative algorithm mainly to save computation time and memory in real-time applications. The NN controller fitted the data well as was shown by the correlation plot. Simulations

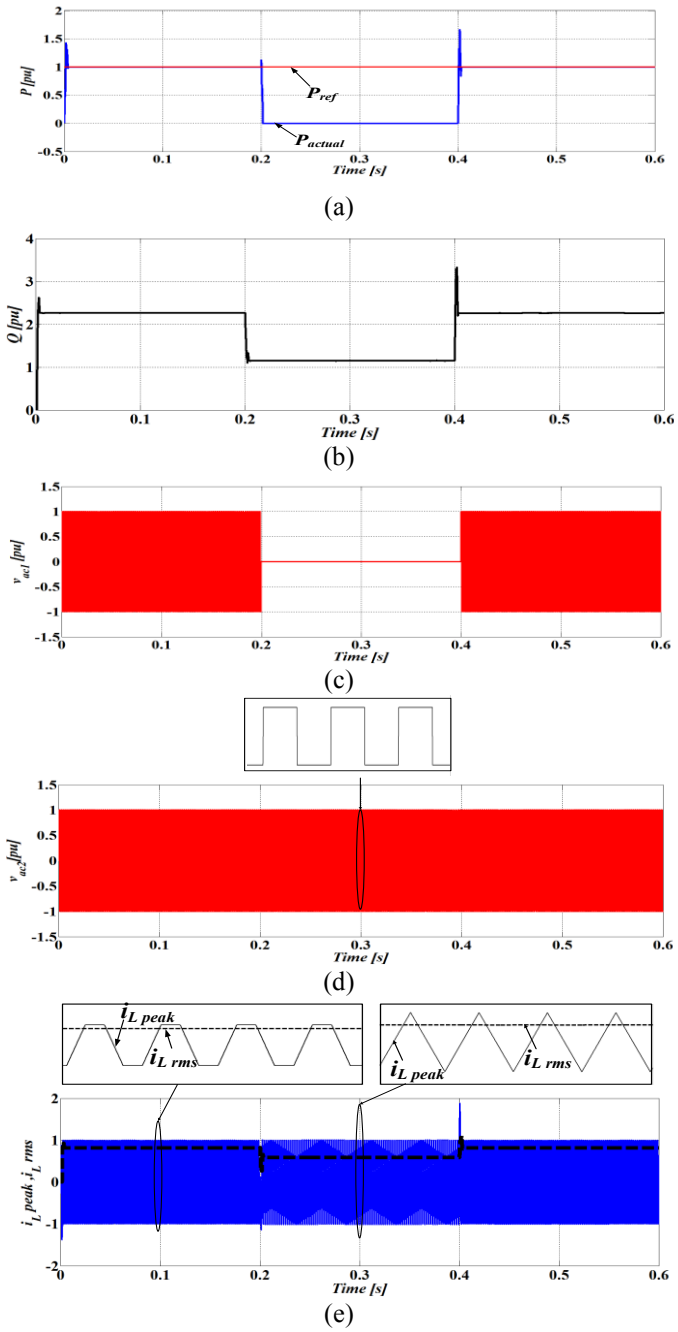

Fig. 10. Converter response under pole to pole DC fault at Bridge 1 (a) reference power vs actual power (b) reactive power (c) Bridge 1 AC voltage (d) Bridge 2 AC voltage, (e) Inductor current

were performed to verify the response of the proposed controller. From the results obtained, the effectiveness of the NN controller under different loading conditions with minimum reactive power selection was demonstrated in addition to its behavior with respect to DC faults.

REFERENCES

[1] Jovcic, D.; Van Hertem, D.; Linden, K.; Taisne, J.-P.; Grieshaber, W., "Feasibility of DC transmission networks," Innovative Smart Grid Technologies (ISGT Europe), 2011 2nd IEEE PES International Conference and Exhibition on , vol., no., pp.1,8, 5-7 Dec. 2011.

[2] Jovcic, D.; Zhang, J., "High power IGBT-based DC/DC converter with DC fault tolerance," Power Electronics and Motion Control Conference (EPE/PEMC), 2012 15th International, vol., 4-6 Sept. 2012.

[3] Tan, N.M.L.; Abe, T.; Akagi, H., "Design and Performance of a Bidirectional Isolated DC–DC Converter for a Battery Energy Storage System," Power Electronics, IEEE Transactions on, vol.27, no.3, pp.1237, 1248, March 2012.

[4] R. W. De Doncker, D. M. Divan, and M. H. Kheraluwala, "A three phase soft-switched high power density DC/DC converter for high power applications," in Conf. Rec. IEEE IAS Annu. Meeting, Pittsburgh, PA,Oct. 2–7, 1988, pp. 796–805.

[5] Krismer, F.; Kolar, J.W., "Accurate Small-Signal Model for the Digital Control of an Automotive Bidirectional Dual Active Bridge," Power Electronics, IEEE Transactions on , vol.24, no.12, pp.2756,2768, Dec. 2009.

[6] Hua Bai; Chunting Mi; Chongwu Wang; Gargies, S., "The dynamic model and hybrid phase-shift control of a dual-active-bridge converter," Industrial Electronics, 2008. IECON 2008. 34th Annual Conference of IEEE, vol., no., pp.2840,2845, 10-13 Nov. 2008.

[7] Segaran, D.; Holmes, D.G.; McGrath, B.P., "Enhanced Load Step Response for a Bidirectional DC–DC Converter," Power Electronics, IEEE Transactions on , vol.28, no.1, pp.371,379, Jan. 2013

[8] Kadavelugu, A.; Seunghun Baek; Dutta, S.; Bhattacharya, S.; Das, M.; Agarwal, A.; Scofield, J., "High-frequency design considerations of dual active bridge 1200 V SiC MOSFET DC-DC converter," Applied Power Electronics Conference and Exposition (APEC), 2011 Twenty-Sixth Annual IEEE , vol., no., pp.314,320, 6-11 March 2011.

[9] R. W. DeDoncker, D. M. Divan, and M. H. Kheraluwala, "A three phase soft-switched high power density DC-to-DC converter for high power applications," IEEE Trans. Industry Applications, vol. 27, no. 1, pp. 63-73, Jan./Feb. 1991.

[10] H. Bai and C. Mi, "Eliminate reactive power and increase system efficiency of isolated bidirectional dual-active-bridge DC-DC converters using novel dual-phase-shift control," IEEE Transactions on Power Electronics, vol. 23, pp. 2905–2914, Nov. 2008.

[11] H. Bai and C. Mi, "Correction to "Eliminate Reactive Power and Increase System Efficiency of Isolated Bidirectional Dual-Active-Bridge DC–DC Converters Using Novel Dual-Phase-Shift Control", IEEE Transactions on Power Electronics, vol. 23, pp. 2905–2914, Sept. 2012.

[12] Biao Zhao; Qingguang Yu; Weixin Sun, "Extended-Phase-Shift Control of Isolated Bidirectional DC–DC Converter for Power Distribution in Microgrid," Power Electronics, IEEE Transactions on , vol.27, no.11, pp.4667,4680, Nov. 2012.

[13] W. Kuiyuan, C. W. de Silva, and W. G. Dunford, "Stability Analysis of Isolated Bidirectional Dual Active Full-Bridge DC-DC Converter With Triple Phase-Shift Control," Power Electronics, IEEE Transactions on, vol. 27, pp. 2007-2017, 2012.

[14] W. Huiqing, and X. Wei dong, "Bidirectional Dual-Active-Bridge DC-DC Converter with Triple-Phase-Shift Control," Applied Power Electronics Conference and Exposition (APEC) 2013, Twenty-Eighth Annual IEEE

[15] H. Wen, "Determination of the optimal sub-mode for bidirectional dual-active-bridge DC-DC converter with multi-phase-shift control," ECCE Asia Downunder (ECCE Asia), 2013 IEEE.

[16] Jain, A.K.; Ayyanar, R., "PWM control of dual active bridge: Comprehensive analysis and experimental verification," Power Electronics, IEEE Transactions on , vol.26, no.4, pp.1215,1227, April 2011.

[17] Garcia, G.O.,Ledhold, R.; Oliva, A.R. ; Balda, J.C. ; Barlow, F. , "Extending the ZVS Operating Range of Dual Active Bridge High-Power DC-DC Converters" IEEE .

[18] Yasen A. Harrye, A.A. Aboushady, K.H. Ahmed and G.P Adam, 'Comprehensive Steady State Analysis of Bidirectional Dual Active Bridge DC/DC Converter Using Triple Phase Shift Control', accepted for publication IEEE ISIE conference, June 2014.

[19] Rahman, M.I.; Jovcic, D.; Ahmed, K.H., "Reactive current optmisation for high power dual active bridge DC/DC converter," PowerTech (POWERTECH), 2013 IEEE Grenoble, vol., no., pp.1,6, 16-20 June 2013.

[20] Mark Hudson Beale, Martin T. Hagan and Howard B. Demuth, "Neural Network Toolbox™ User's Guide", The MathWorks, Inc. 2014a.

[21] MacKay, D.J.C., "Bayesian interpolation," *Neural Computation*, Vol. 4, No. 3, 1992, pp. 415–447.

[22] Hagan, M.T.; Menhaj, M.-B., "Training feedforward networks with the Marquardt algorithm," *Neural Networks, IEEE Transactions on*, vol.5, no.6, pp.989,993, Nov 1994.